DOI: 10.1002/chem.200801247

Hybrid Host–Guest Complexes: Directing the Supramolecular Structure through Secondary Host–Guest Interactions

Carsten Streb, Thomas McGlone, Oliver Brücher, De-Liang Long, and Leroy Cronin*[a]

Abstract: A set of four hybrid host–guest complexes based on the inorganic crown ether analogue $[H_{12}W_{36}O_{120}]^{12-}$ ($\{W_{36}\}$) have been isolated and characterised. The cluster anion features a central rigid binding site made up of six terminal oxygen ligands and this motif allows the selective binding of a range of alkali and alkali-earth-metal cations. Here, the binding site was utilised to functionalise the metal oxide-based cavity by complexing a range of protonated primary amines within the recognition site. As a result, a set of four hybrid organic–inorganic host–guest complexes were obtained whereby the interactions are highly directed specifically within this cavity. The guest cations in these molecular assemblies range from the aromatic 2-phenethylamine (**1**) and 4-phenylbutylamine (**2**) to the bifunctional aromatic *p*-xylylene diamine (**3**) and the aliphatic, bifunctional 1,6-diaminohexane (**4**). Compounds **1**–**4** were structurally characterised by single-crystal X-ray diffraction, elemental analysis, flame atomic absorption spectroscopy, FTIR and bond valence sum calculations. This comparative study focuses on the supramolecular effects of the amine guest cations and investigates their structure-directing effects on the framework arrangement arising by locking the protonated amines within the cavity of the $\{W_{36}\}$ cluster. It was shown that parts of the organic guest cation protrude from the central binding cavity and the nature of this protruding organic "tail" directs the solid-state arrangement of compounds **1**–**4**. Guest cations with a hydrophobic phenyl tail result in an antiparallel assembly of $\{W_{36}\}$ complexes arranged in a series of pillared layers. As a consequence, no direct supramolecular interactions between $\{W_{36}\}$ clusters are observed. In contrast, bifunctional guest cations with a secondary amino binding site act as molecular connectors and directly link two cluster units thus locking the supramolecular assembly in a tilted arrangement. This direct linking of $\{W_{36}\}$ anions results in the formation of an infinite supramolecular scaffold.

Keywords: crown compounds · host–guest systems · hybrid materials · self-assembly · supramolecular chemistry

Introduction

Polyoxometalates (POMs) are polynuclear metal–oxide clusters formed by the self-assembly of oxo-anions of molybdenum, tungsten or vanadium.[1] A vast range of structural types is accessible with nuclearities ranging from 6 to 368 metal centres. Tungsten[2] and molybdenum-based[3] systems in particular have been subjected to a vast number of studies due to their attractive electronic and molecular properties, making these clusters ideal candidates for applications in catalysis,[5,6] magnetism,[7,8] electron-transfer processes,[9,10] materials science[11–13] and medicine.[14,15] Typically, the synthesis of polyoxometalates employs "one-pot" reactions in which a multitude of parameters, such as acidity, ionic strength of the solvent, temperature and pressure, dramatically affect the final product. The manipulation of a single reaction parameter can, therefore, represent a facile but serendipitous route to novel POM architectures. However, the predetermined assembly of complex cluster systems by using smaller, well-known building blocks still represents a major challenge, and the successful implementation of this approach could provide direct control over the cluster architectures and the physical properties of the materials. It is this prospect that over the last decade has sparked a tremendous amount of research into the self-assembly of POM-based secondary building blocks.[16] The utilisation of readily available POM building blocks as synthons in the designed assembly of more complex systems could allow a

[a] Dr. C. Streb, T. McGlone, O. Brücher, Dr. D.-L. Long, Prof. L. Cronin
WestCHEM, Department of Chemistry
The University of Glasgow
Glasgow G12 8QQ (UK)
Fax: (+44) 141-330-4888
E-mail: L.cronin@chem.gla.ac.uk

more controlled way of forming clusters with novel functionalities. In addition, this approach would allow the systematic control of the overall cluster architecture whilst retaining the geometries of the synthons. The major challenge of this approach is the identification of reactive building blocks that can be obtained in solution at concentrations that allow the formation of more complex architectures without undergoing spontaneous rearrangement or isomerisation processes.[17–22]

Recently, we have identified one facile route that allows the stabilisation of reactive building blocks in solution and indeed resulted in the isolation of novel cluster types in the solid state. Bulky organic cations were used to kinetically stabilise and encapsulate metastable intermediates and prevent further rearrangement into thermodynamically favoured, well-known structures.[17–20] By using this approach, a highly charged low-symmetry $\{Mo_{16}\}$ unit, $[H_2Mo^{V}_4Mo^{VI}_{12}O_{52}]^{10-}$, was previously isolated.[21] The $\{Mo_{16}\}$ cluster is stable in the solid state and it was shown that the highly negative anion is virtually completely wrapped by the organic counterions. Importantly, this approach can be extended towards other cluster families, for example, in the development of sulfite-based Dawson-type mixed-valence polyoxomolybdates $[Mo_{18}O_{54}(SO_3)_2]^{n-}$, by using the same type of synthetic approach.[23,24] Thus, the use of bulky organic cations in the formation of Mo-based POMs appears to restrict aggregation to the more highly symmetrical cluster types, allowing a fundamentally more diverse set of clusters and cluster-based building blocks to be isolated, that display unprecedented structural[21,22] or physical[23] features. This observation was explored further when we used bulky organocations to help isolate and connect $\{Mo_8Ag_2\}$ building blocks into larger polymeric architectures.[25,26]

The extension of this approach to isopolyoxotungstates[27,28] has also proved important in allowing us to isolate a family of $\{W_{36}\}$-based host–guest complexes[29,30] with the generic formula $M\subset[H_{12}W_{36}O_{120}]^{n-}$ ($M = K^+$, Rb^+, Cs^+, NH_4^+, Sr^{2+}, Ba^{2+}) that incorporate a rigid crown ether like POM-based binding site (Figure 1). The $\{W_{36}\}$ itself is assembled from three $\{W_{11}\}$ ψ-metatungstate units[27,28] that are linked by a set of three connecting $[WO_6]$ octahedra so that the overall structure can be rationalised as $\{W_{36}\} = \{W_{11}\}_3\{W_1\}_3$ (Figure 1).

This $\{W_{36}\}$ cluster represents the largest isopolyoxotungstate so far discovered and can be described as a ring-shaped unit that features a metal–oxo framework, which resembles the [18]crown-6 ether.[31] $\{W_{36}\}$ shows further similarities to crown ethers, for instance, the ability to bind alkali and alkali-earth-metal as well as ammonium cations in the central binding pocket of the cluster. The results obtained so far strongly suggest that the cluster assembly is driven by the presence of a central templating cation that allows the arrangement of the building blocks into the ring-shaped $\{W_{36}\}$ anion. In fact, it has been shown that the $\{W_{36}\}$ cluster can only be obtained in the presence of templating cations. This can be clearly shown when a range of alkali and alkali-earth-metal cations were employed as guests and gave a number of $\{W_{36}\}$-based host–guest complexes.[29,30] Subsequent synthetic efforts showed that the central guest position can also be occupied by ammonium cations that bind to the cavity by means of electrostatic interactions and hydrogen bonding.[30] Inspired by these results, the formation of truly hybrid organic–inorganic assemblies was attempted by employing protonated primary amines as guests so as to mimic the binding behaviour of the inorganic ammonium cation.

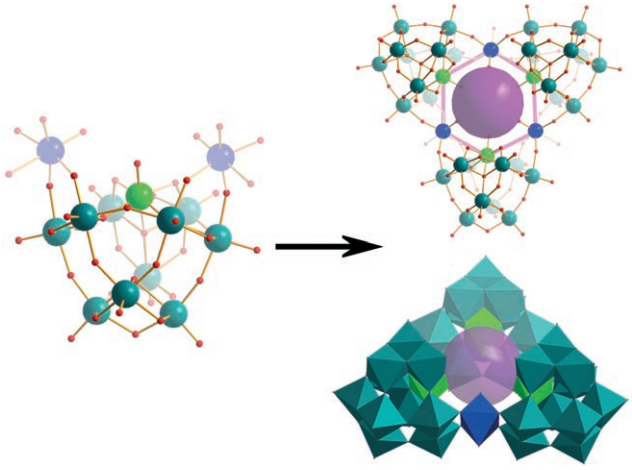

Figure 1. Illustration of the formal self-assembly of the $\{W_{36}\}$ cluster shell $[H_{12}W_{36}O_{120}]^{12-}$. Left: The ψ-metatungstate cluster $[H_2W_{11}O_{38}]^{8-}$ (green) with two $\{W_1\}$ connectors (blue). The W centre that is part of the binding pocket is highlighted in light green. Right: Top view and side view of the self-assembly of three ψ-metatungstate units (green) and three $\{W_1\}$ octahedra (blue) to give the ring-shaped $\{W_{36}\}$ cluster. The central binding pocket (purple) is created by six terminal oxygen atoms located on the $\{W_{11}\}$ (light green) and $\{W_1\}$ units (blue). O: red spheres.

Here, we report four hybrid $\{W_{36}\}$-based compounds in which protonated organic amines were used as guest molecules that interact with the central binding site of the cluster anion through their terminal ammonium groups. The use of the phenyl-terminated amines phenethyl amine **1** and 4-phenylbutyl amine **2** resulted in the formation of non-connected molecular host–guest systems, whereas the bifunctional amines *p*-xylylene diamine **3** and 1,6-diaminohexane **4** gave directly linked hybrid host–guest scaffolds, and are interesting because the binding site, located within the cavity, ensures that the interactions are highly directed, which enables the prospect of real design approaches to the development of hybrid structures with nanoscale POM cluster units.

Results and Discussion

Description of the $\{W_{36}\}$ cluster framework: The tungsten–oxo frameworks of the $\{W_{36}\}$ units found in compounds **1** to **4** are virtually identical and can thus be discussed at this stage by using one representative example. The $\{W_{36}\}$ cluster features an idealised C_{3v}-symmetric tungsten–oxide shell and comprises three $\{W_{11}\}$ cluster subunits linked together by three $\{W_1\}$ bridges. The $\{W_{11}\}$ ψ-metatungstate units[27,28]

consist of a ring of six apical W positions, an additional W position in the centre of this ring and four basal W positions in a butterfly configuration. Two protons are present at the centre of the $\{W_{11}\}$ unit and form hydrogen bonds between the four internal bridging oxo ligands.[27,28] Three $\{W_1\}$ units act as linkers between the $\{W_{11}\}$ fragments by sharing four bridging oxo ligands in the equatorial plane. In addition, the $\{W_1\}$ bridges feature one water ligand ($d_{W-H2O} \approx 2.3$ Å) that points away from the cluster centre. The nature of this ligand was also supported by bond valence sum calculations (BVS), which indicate a low-bond valence characteristic for this type of ligand. All 36 W centres have a distorted $[WO_6]$ octahedral coordination geometry with one terminal W=O ($d_{W=O} \approx 1.7$ Å) group extending away from the cluster surface. This feature is typical for tungsten centres in the oxidation state +VI. The central binding site is formed by six terminal oxygen ligands that are split into two groups. Every $\{W_{11}\}$ unit features one terminal oxo ligand extending away from its apex into the central cavity. In addition, each of the $\{W_1\}$ linkers features one oxygen donor that also points towards the central vacancy, so that a hexagonal array of six oxygen sites is created. The six oxo donors do not adopt a planar arrangement; instead they are alternatively offset above or below the mean plane of the $\{W_{36}\}$ unit. This rigid arrangement results in the formation of a negatively polarised central binding site that is ideally suited for positively charged hydrogen-bonding guest molecules (Figure 1).

Structural description of the host–guest complexes 1–4: The structures of compounds **1–4** were determined by using single-crystal X-ray diffraction (Table 1).[32] In compound **1**, protonated phenethyl amine $Ph(C_2H_4)NH_3^+$ (PEA) was introduced to the $\{W_{36}\}$ reaction mixture and structural analysis of the crystalline product **1** gave the formula $(TEAH)_{11}\{(Ph(C_2H_4)NH_3) \subset [H_{12}W_{36}O_{120}]\} \cdot ca.17\,H_2O$ ($(TEAH)_{11}$**1a**$\cdot ca.17\,H_2O$). The crystallographic data showed that a $\{W_{36}\}$-based host–guest complex was obtained that featured protonated PEA cations as guest molecules within the $\{W_{36}\}$ central binding pocket. The positively charged ammonium group of the PEA cation is held in place by ion-dipole electrostatic interactions with the six oxo donors of the binding site (Figure 2). In addition, the ammonium group can form hydrogen bonds with three of the oxo li-

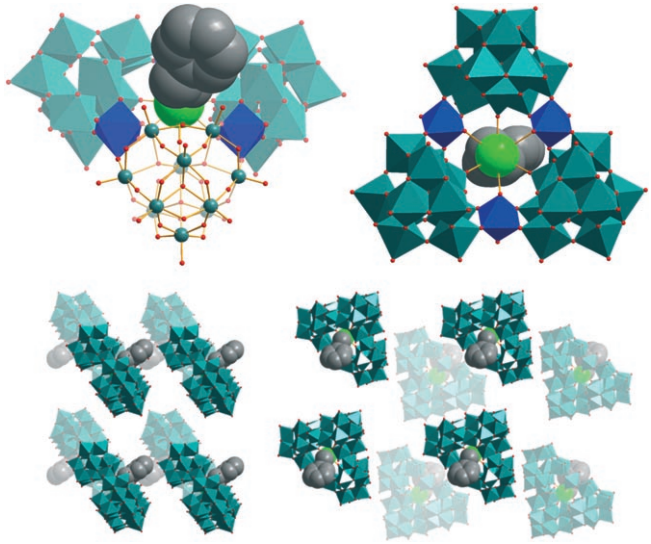

Figure 2. Top: Side view (left) and top view (right) of the host guest complex **1a**, PEA$\subset[H_{12}W_{36}O_{120}]$. The top view illustrates the binding mode of the primary amine of the ligand $Ph(C_2H_4)NH_3^+$ that interacts with the central ring of six W=O terminal oxygen sites. The side view illustrates the protruding organic substituent that is located in one hemisphere of the $\{W_{36}\}$ ring. Colour scheme: $\{W_{11}\}$: green, $\{W_1\}$ linkers: blue, O: red, N: green, C: grey. Bottom: Illustration of the framework arrangement of **1**. The side-on view (left) and the top view (right) highlight the antiparallel arrangement between neighbouring layers of $\{W_{36}\}$ units. Colour scheme: $\{W_{11}\}$: green, $\{W_1\}$ linkers: blue, $\{W_{36}\}$: green O: red, N: green, C: grey. Water molecules and TEAH counterions are omitted for clarity.

Table 1. Crystallographic data for compounds **1–4**.

	1	**2**	**3**	**4**
formula	$C_{74}H_{234}N_{12}O_{170}W_{36}$	$C_{76}H_{238}N_{12}O_{170}W_{36}$	$C_{62}H_{204}N_{11}Na_1O_{164}W_{36}$	$C_{60}H_{208}N_{11}NaO_{164}W_{36}$
M_r [g mol^{-1}]	10631.33	10598.92	10369.49	10349.50
crystal system	triclinic	monoclinic	orthorhombic	orthorhombic
space group	$P\bar{1}$	$P21/c$	$Pnma$	$Pnma$
a [Å]	21.2201(6)	20.8527(8)	26.9515(12)	27.1753(2)
b [Å]	21.3592(8)	35.4301(14)	35.2430(15)	35.0988(3)
c [Å]	25.3862(8)	27.2308(10)	21.4907(10)	21.2024(2)
α [°]	95.793(2)	90	90	90
β [°]	91.268(2)	93.393(2)	90	90
γ [°]	95.597(2)	90	90	90
ρ_{calcd} [g cm^{-3}]	3.101	3.525	3.381	3.407
V [Å^3]	11386.9(6)	20083.2(13)	20413.0(16)	20223.0(3)
Z	2	4	4	4
$\mu(Mo_{K\alpha})$ [mm^{-1}]	18.203	20.642	20.305	20.495
T [K]	150(2)	100(2)	150(2)	100(2)
no. rflns (measd)	112861	151007	83614	71598
no. rflns (unique)	35295	37929	16708	14838
no. params	2332	2183	1110	1109
$R1$ ($I > 2\sigma(I)$)	0.0544	0.0469	0.0384	0.0339
$wR2$ (all data)	0.1407	0.1119	0.0946	0.0784

gands, resulting in two distinct N···O interactions. Short, hydrogen-bonded N···O distances of approximately 2.77 Å were observed between the nitrogen and the three terminal oxygen sites located on the $\{W_{11}\}$ fragments. In contrast, the N···O interactions with the oxygen ligands located on the $\{W_1\}$ linking units are elongated to approximately 3.25 Å, thus suggesting purely electrostatic long-range interactions.

One major feature of the organo-substituted host–guest system **1a** is the organic phenyl "tail" that is protruding from the central cavity. As a result, the phenyl ring of the PEA ligand is located on one discrete hemisphere of the $\{W_{36}\}$ cluster and only the sterically favoured positional isomer is obtained. The effect of the bulky organic substituent on the binding mode within the central cavity can be examined by comparison of the distance between the nitrogen centre of the PEA ligand and the mean plane formed by the six oxygen atoms of the binding site. In **1a**, the nitrogen atom is displaced from the mean complexation plane by $d_{N\text{–centre}} = 1.22$ Å, whereas the sterically non-hindered parent compound, $NH_4 \subset \{W_{36}\}$, features a separation of $d_{N\text{–centre}} = 0.97$ Å.[30]

The effect of these protruding tails on the solid-state arrangement of compound **1** was investigated by analysis of the packing in the crystal lattice. The dominating structural feature in the solid state is the ABAB-type layered arrangement of the hybrid $\{W_{36}\}$ units. Each layer A features a set of $\{W_{36}\}$ anions aligned in a parallel fashion so that the organic tails point in the same direction; the next layer B features an antiparallel orientation of the host–guest complexes so that all phenyl tails in layer B point in the opposite direction of the tails in layer A. In effect, a non-polar crystal lattice is obtained (Figure 2). Both, the inter- and intralayer interactions between $\{W_{36}\}$ units are restricted because the organic phenyl tails act as hydrophobic barriers that inhibit any supramolecular interactions with adjacent clusters. Thus the host–guest complexes **1a** are obtained as non-connected molecular species with minimum intercluster spacings of 4.77 Å. The cluster anions are encapsulated by protonated TEAH cations that reinforce the structure by electrostatic and hydrogen-bonding interactions. Furthermore, compound **1** contains a complex network of hydrogen-bonded water molecules that interact with both the cluster anions and the TEAH molecules.

In the next set of experiments, a simple guest substitution approach was chosen to investigate the feasibility of replacing the phenethyl ammonium cation with longer alkyl-chain analogues, such as protonated 4-phenylbutyl amine ($Ph\text{-}(CH_2)_4NH_3^+$) (4PBA). The addition of 4PBA to the $\{W_{36}\}$ reaction mixture led to the isolation of compound **2**, $(TEAH)_{11}\{4PBA \subset [H_{12}W_{36}O_{120}]\} \cdot ca.17\,H_2O$ ($(TEAH)_{11}$**2a**$\cdot ca.17\,H_2O$). Structural analysis reveals striking similarities between the host–guest anion **2a**, $4PBA \subset [H_{12}W_{36}O_{120}]$, and the cluster anion **1a**. The 4PBA ligand is located in the binding site of the $\{W_{36}\}$ framework, docked on through the protonated primary amine function of the guest cation. A combination of electrostatic and hydrogen-bonding interactions are formed so that the ammonium group is engaged in two sets of N···O interactions. Short range, hydrogen-bonded N···O interactions are established to the $\{W_{11}\}$-based terminal oxygen sites with average N···O distances of approximately 2.80 Å. Long-range electrostatic interactions are observed between the nitrogen centre and the $\{W_1\}$-based oxygen donors with typical distances of $d_{N\cdots O} \approx 3.30$ Å. The displacement of the 4PBA ligand from the cluster centre is marginally larger in **2a**, with a spatial separation of $d_{N\cdots centre} = 1.32$ Å (relative to ca. 1.22 Å for PEA and ca. 0.97 Å for NH_4^+). The organic tail protrudes from this central cavity and is located in one hemisphere of the $\{W_{36}\}$ unit resulting in the formation of only one positional isomer (Figure 3).

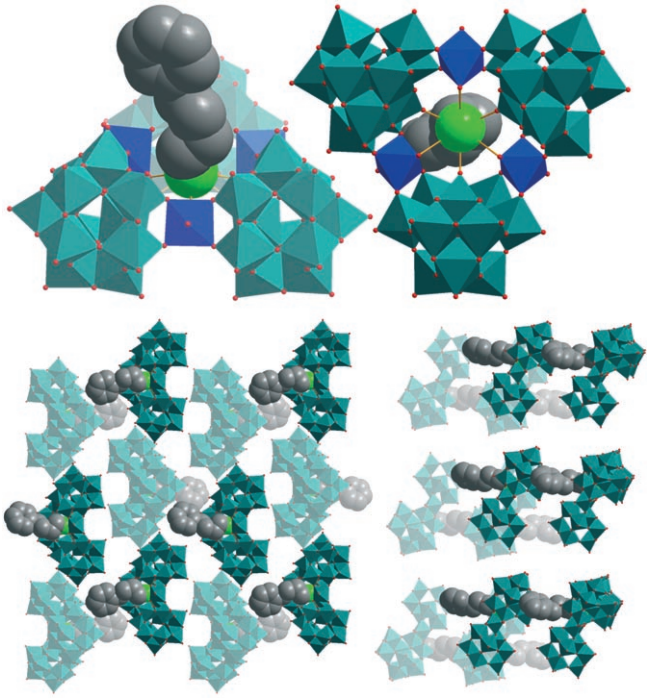

Figure 3. Side view (top left) and top view (top right) of the $\{W_{36}\}$-based cluster anion **2a**, $4PBA \subset [H_{12}W_{36}O_{120}]$. The location of the organic ligand 4PBA in the centre of the binding pocket is illustrated. Detailed structural analysis shows that the ligand is displaced so that the nitrogen centre is located above the mean binding plane of the $\{W_{36}\}$ host. The top view shows that the amino group is located centrally within the equatorial binding plane and forms hydrogen bonds to the oxygen donors. View of the crystal lattice of **2** along the crystallographic *a* axis (bottom left) and *b* axis (bottom right). The protruding 4PBA ligands are highlighted by a space-filling representation to emphasise their supramolecular effect on the crystal packing. By alternatively pointing towards the same intercluster voids, the ligands create a layered arrangement that is pillared by TEAH counterions and water molecules (omitted for clarity). $\{W_{36}\}$: green polyhedra, C: grey, N: green, O: red.

The supramolecular packing of compound **2** features layers of host–guest complexes that are arranged in an ABAB-type antiparallel fashion and is, therefore, comparable to the packing in compound **1**. The assembly of $\{W_{36}\}$ anions into layers is governed by the protruding organic phenyl tails that are pairwise aligned so that, in effect, a pil-

laring of the host–guest compounds is achieved. It is interesting to note that the organic substituents that protrude from the binding sites are aligned in an almost parallel fashion; however, adjacent phenyl rings are too far apart to interact by means of π–π stacking, as the bulky $\{W_{36}\}$ rings do not allow a closer packing (Figure 3). In the crystal lattice, no direct cluster-to-cluster supramolecular interactions are observed and the $\{W_{36}\}$ anions **2a** are isolated as non-connected molecular units. It is interesting to note that the larger 4PBA ligand does not affect the intercluster distance. For compound **2**, the minimum distance between two cluster anions is 4.55 Å, whereas for compound **1**, the minimum distance observed is 4.77 Å. This suggests that the main influence on the close packing of the $\{W_{36}\}$ units is not the size of the guest cation, but the large number of organic TEAH counter ions that encapsulate the clusters and form a stabilizing complex network of hydrogen bonds with additional solvent water molecules.

To exploit the potential of the $\{W_{36}\}$ system further and to examine the compatibility of bifunctional molecules with the $\{W_{36}\}$ host anion, diprotonated *p*-xylylene diamine, *p*-$(CH_2{-}NH_3)_2C_6H_4^{2+}$ (*p*XDA) was employed to introduce a secondary interaction site. The reaction of *p*XDA with an acidified sodium tungstate solution at pH 2.2 under the standard $\{W_{36}\}$ reaction conditions yielded a crystalline product, compound **3**. The material was characterised by single-crystal X-ray diffraction and structural analysis revealed the formula as $(TEAH)_8Na_2\{p\text{XDA}\subset[H_{12}W_{36}O_{120}]\}\cdot ca.17H_2O$ ($(TEAH)_8Na_2$**3a**$\cdot ca.17H_2O$). In **3a**, one ammonium group of the *p*XDA ligand is located in the central $\{W_{36}\}$ binding site in a similar fashion to that observed for the monoamines in **1a** and **2a**. Due to the non-planar arrangement of the six binding oxo-ligands within the central pocket, the $\{W_{11}\}$-based oxygen atoms in the **3a** form are engaged in electrostatic and hydrogen-bonding interactions with the *p*XDA nitrogen centre. As a result, short N···O distances of approximately 2.78 Å are observed. The oxygen donors located on the $\{W_1\}$ linking units are engaged in long-range electrostatic interactions with the ammonium function and are separated by long N···O distances of approximately 3.29 Å. As a consequence of this binding mode, the ammonium group is displaced from the equatorial plane of the $\{W_{36}\}$ host by approximately 1.30 Å, which is in line with the structures discussed earlier. The *p*XDA diamine protrudes from the cluster cavity and is located in one hemisphere of the $\{W_{36}\}$ host anion (Figure 4).

With regard to the supramolecular structural arrangement of the anions in the crystal lattice of **3**, a distinctive effect of the *p*XDA ligand can be observed. The $\{W_{36}\}$ host–guest complexes in compound **3** do not assemble in an antiparallel fashion as the organo-derivatives **1** and **2**; instead they adopt a tilted ABAB-type pattern resulting in two layers of $\{W_{36}\}$ anions with a torsion angle of approximately 76.2°. This pattern closely resembles the crystal lattices found in the purely inorganic compounds $M\subset\{W_{36}\}$. The archetypal compound $K\subset\{W_{36}\}$, for example, features an interlayer torsion angle of approximately 79.2°.[29,30] The formation of this

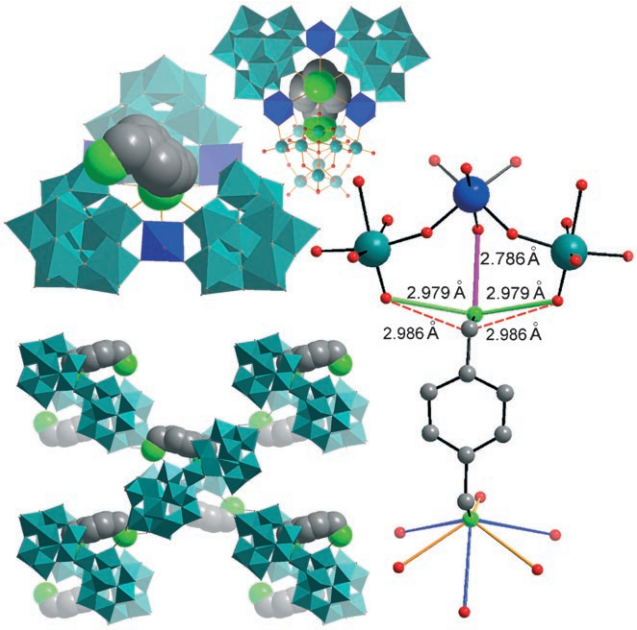

Figure 4. Top: Polyhedral representation of host–guest complex **3a**, *p*XDA⊂$\{W_{36}\}$. The side view (left) illustrates the protruding *p*-xylylene diamine ligand with the peripheral ammonium group, which can engage in further supramolecular interactions. The top view (right) highlights the location of the organic ligand within the binding pocket of the $\{W_{36}\}$ host anion. Bottom: View along the crystallographic *b* axis of **3** *p*XDA⊂$\{W_{36}\}$ (left), illustrating the connection mode between the bifunctional organic amine *p*XDA and two adjacent $\{W_{36}\}$ cluster anions. The organic cation binds to the central cavity of one $\{W_{36}\}$ host and establishes hydrogen-bonding interactions to an adjacent cluster "locking" the two clusters in a tilted arrangement. The detailed view of the interactions of the *p*XDA ligand (right) illustrates the binding of one amine to the central $\{W_{36}\}$ binding pocket (bottom) through long (blue) and short (orange) hydrogen-bonded N···O interactions. The supramolecular interactions of the pendant amine arm (top) highlight the two hydrogen-bonded N···O interactions (magenta and green) and the CH···O interactions (red dashed line). $\{W_{11}\}$ fragment: green, $\{W_1\}$ linker: blue, O: red, N: green, C: grey.

supramolecular assembly is facilitated by the protruding *p*XDA ligands, which form strong interactions to adjacent $\{W_{36}\}$ units through the peripheral protonated ammonium group. In detail, the pendant NH_3^+ group interacts with three terminal oxo ligands located on the cluster shell of a neighbouring $\{W_{36}\}$ unit through electrostatic and hydrogen-bonding interactions. The shortest N···O bond is observed between the protonated amine and the coordinating water ligand on the outside of the $\{W_1\}$ linking unit ($d_{N\cdots O}$ = 2.786(5) Å). This suggests strong, hydrogen-bonding interactions since both the amine and the water ligand can act as hydrogen-bond donors. Furthermore, two hydrogen bonds to the $\{W_{11}\}$ subunits on either side of the $\{W_1\}$ linker are observed that feature slightly elongated N···O distances of $d_{N\cdots O}$ = 2.979(4) Å. It is noteworthy that this spatial arrangement allows for close contacts between the α-methylene group of the *p*XDA ligand and the $\{W_{11}\}$ terminal oxygen atoms so the formation of CH···O hydrogen bridges is likely ($d_{C\cdots O}$ = 2.986(3) Å). These are, however, driven by sterical necessity and are not expected to direct this assembly.

In essence, the *p*XDA group acts as a ditopic linker that connects two adjacent $\{W_{36}\}$ anions by docking onto the central binding pocket of one $\{W_{36}\}$ host and further establishing a link to the periphery of a second $\{W_{36}\}$ anion through the pendant ammonium group. This set of directed interactions enables the clusters to adopt the tilted packing mode described above (Figure 4). Further framework stabilisation is provided by the presence of a coordinating sodium cation that is located on the periphery of each $\{W_{36}\}$ anion and that interacts with TEAH cations through hydroxyl coordination bonds. This motif in combination with further non-coordinating TEAH ligands and water molecules results in the formation of a vast hydrogen-bonded network that reinforces the structural stability of compound **3**.

To study the versatility of this linking approach, a suitable diprotonated aliphatic diamine, 1,6-diaminohexane (DAH), was introduced to the reaction system and resulted in the isolation of a crystalline product, compound **4**. Structural analysis was accomplished by single-crystal XRD and revealed the composition $(TEAH)_8Na_2\{DAH\subset[H_{12}W_{36}O_{120}]\}\cdot ca.17H_2O$ ($(TEAH)_8Na_2$**4a**$\cdot 17H_2O$). Investigation of the crystal structure showed that a diprotonated 1,6-diaminohexane molecule was located in the centre of the $\{W_{36}\}$ coordination cavity (Figure 5). The binding mode adopted by the DAH ligand in **4a** can be compared to the binding situation in **3a**. One terminal ammonium function binds to the central

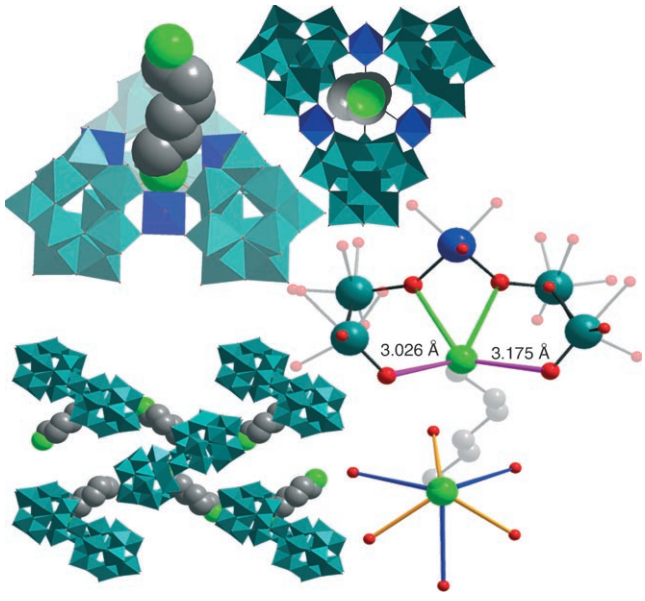

Figure 5. Top: Side view (left) and top view (right) of the cluster anion **4a**, DAH⊂$\{W_{36}\}$. Bottom: Left: View along the crystallographic *b* axis of **4**, illustrating the connectivity between adjacent $\{W_{36}\}$ cluster anions. The organic cation binds to the central cavity of one $\{W_{36}\}$ host and in addition binds to the periphery of a neighbouring $\{W_{36}\}$ unit, resulting in the stabilisation of the tilted arrangement. Right: Detailed illustration of the connectivity mode of the DAH ligand. One ammonium moiety binds to the central $\{W_{36}\}$ binding site (bottom) through long (blue) and short (orange) N···O interactions. The pendant ammonium group (top) forms short contacts to four oxo ligands on a neighbouring $\{W_{36}\}$ cluster unit (magenta and green). $\{W_{11}\}$ fragment: green, $\{W_1\}$ linker: blue, O: red, N: green, C: grey.

binding pocket and forms two distinct N···O interactions with the two sets of oxygen donors on the $\{W_{36}\}$ framework. Short hydrogen-bonded N···O distances of approximately 2.80 Å are observed for interactions with the oxygen atoms based on the $\{W_{11}\}$ subunits, whereas elongated N···O spacings of approximately 3.33 Å were found for the $\{W_1\}$-based terminal oxo ligands. As a result of these interactions, the DAH cation is displaced from the cavity centre by 1.33 Å, which is in line with the compounds discussed earlier. Further, this suggests that the steric strain introduced by the bulky phenyl rings in the compounds **1, 2** and **3** is comparatively low. It should be noted that in the crystal structure of **4**, the C_6 chain of the DAH ligand is disordered over two sites. The overall arrangement of the ligand, however, is not affected because the two terminal ammonium functions are located in well-defined positions and thus lock the molecule in a given orientation.

In the crystal lattice, the $\{W_{36}\}$ cluster units are positioned in an ABAB fashion similar to the situation discussed above for compound **3**. The $\{W_{36}\}$ clusters in **4** form two distinct layers and feature a torsion angle of approximately 76.9° relative to their respective equatorial planes. The organic DAH ligand supports this arrangement by docking onto the adjacent cluster anion with a pendant protonated amino function, thus acting as a supramolecular linking unit. In detail, the protruding amino group establishes four short hydrogen-bonded N···O interactions (Figure 5). The shortest N···O distance is formed between the pendant nitrogen centre and two μ_2-bridging oxygen ligands that connect the $\{W_1\}$ linker unit with the $\{W_{11}\}$ fragment ($d_{N\cdots O}=3.026(3)$ Å). This close contact results in the formation of two symmetry-related supramolecular interactions. Slightly longer N···O distances are observed between the nitrogen atoms and two terminal oxygen ligands located on the $\{W_{11}\}$ subunit. As a result, the DAH ligand connects two $\{W_{36}\}$ units in very much the same way as discussed previously for the *p*XDA ligand in compound **3**, that is, by the combination of binding to the central $\{W_{36}\}$ cavity and additional hydrogen-bonding interactions with a neighbouring cluster unit (Figure 5).

It is noteworthy that the close relationship between the solid state arrangement of the cluster anions in **3** and **4** and the purely inorganic compounds reported earlier[29,30] is also reflected by their crystallographic properties. All inorganic compounds are isostructural and crystallise in the orthorhombic space group *Pnma* with unit-cell dimensions of approximately 27 (*a*), 35 (*b*) and 21 Å (*c*) and only differ in the arrangement of the organic counterions. This trend is also observed in compounds **3** and **4**, which also feature the orthorhombic space group *Pnma* with virtually identical unit-cell dimensions. In contrast, compounds **1** and **2** crystallise in lower-symmetry space groups as their monofunctional organic guest cations do not support the arrangement in the original tilted orientation.

Conclusion

A designed approach has been presented that allowed the organic functionalisation of the formerly pure inorganic host–guest complexes M⊂{W_{36}} ($M = K^+$, Rb^+, Cs^+, Sr^{2+}, Ba^{2+}, NH_4^+) by using protonated organic amines. This modification is vital because it allows the direct linking of the clusters through the guest cation. In effect, ditopic guest molecules can act as connectors between {W_{36}} host anions and might, in future, allow the assembly of a family of interconnected {W_{36}}-based frameworks. The working principles for this approach have been demonstrated and two distinctive effects of these organic ligands on the supramolecular assembly of the {W_{36}} host–guest system have been established. The phenyl-terminated monoamines in compounds **1** and **2** effectively act as hydrophobic "bumpers" that prohibit close contacts and thus direct supramolecular interactions between adjacent cluster groups in the crystal lattice. It is this that allows the formation of TEAH-encapsulated molecular units that do not engage in direct contacts with neighbouring {W_{36}} clusters. In contrast, the introduction of a secondary binding site in compounds **3** and **4** resulted in the direct linkage of adjacent {W_{36}} clusters by virtue of the second amino function on the bifunctional ligand. This feature enabled the diamines to interact with the central binding pocket of one {W_{36}} host while also binding to the periphery of the neighbouring cluster. In effect, this binding mode resulted in the formation of a supramolecular organic–inorganic scaffold. Future work will further exploit the potential of these hybrid systems and will explore the possibility of introducing diamines that can directly interact with two central {W_{36}} binding pockets.

Experimental Section

General: All reagents and chemicals were purchased from Sigma-Aldrich and were used without further purification. Elemental Analyses were performed by using a Perkin–Elmer Elemental Analyzer CHN2000. It should be noted that the material contains a large amount of disordered organic TEAH counterions and water of crystallisation that had to be estimated from elemental analyses and charge-balance calculations.[30] However, this did not affect the characterisation and analysis of the cluster anions. FTIR spectroscopy was carried out by using a JASCO FTIR 410 spectrometer and wavenumbers are given in cm^{-1}. Intensities are denoted as vs = very strong, s = strong, m = medium, w = weak and br = broad. Single-crystal X-ray crystallography diffraction data were collected on a Bruker Apex II CCD Diffractometer. SHELXS-97 was used for structure solution and SHELXL-97 was used for full least-squares refinement on F^2.[32]

Compound 1 ($(TEAH)_{11}\{(Ph(C_2H_4)NH_3)\subset[H_{12}W_{36}O_{120}]\}\cdot ca.17H_2O$): $Na_2WO_4\cdot 2H_2O$ (2.00 g, 6.06 mmol) and triethanolamine hydrochloride (2.5 g, 13.47 mmol) were dissolved in H_2O (50 mL) and the pH was adjusted to 2.2 by using HCl (ca. 2 mL, 4 M). After heating the reaction mixture to approximately 80–85 °C in a microwave, phenethylamine (29 mg, 0.24 mmol) dissolved in H_2O (5 mL) was added dropwise to the stirred hot solution and the mixture was allowed to cool down to room temperature. The clear colourless solution was kept in a plastic vial and after approximately 1 week large colourless crystalline rhombohedra of **1** were isolated. The crystals were collected on a filter paper, washed with cold water and dried. Yield: 0.867 g (82 μmol, 48.7% based on W); characteristic IR bands: $\tilde{\nu} = 3425$ (m,br), 3058 (w), 1601 (w), 1444 (w), 1351 (w), 1212 (w), 1088 (w), 1051 (vs), 982 (vs), 948 (vs), 888 (vs), 771 cm^{-1} (s); elemental analysis calcd (%) for $C_{74}H_{234}N_{12}O_{170}W_{36}$: C 8.36, H 1.91, N 1.47, W 61.81; found: C 8.48, H 2.21, N 1.58, W 62.32.

Compound 2 ($(TEAH)_{11}\{(Ph(C_4H_8)NH_3)\subset[H_{12}W_{36}O_{120}]\}\cdot ca.17H_2O$): $Na_2WO_4\cdot 2H_2O$ (2.00 g, 6.06 mmol) and triethanolamine hydrochloride (2.5 g, 13.47 mmol) were dissolved in H_2O (50 mL). The solution pH was adjusted to 2.2 by using HCl (ca. 2 mL, 4 M). After heating the reaction mixture to approximately 80–85 °C in a microwave, 4-phenylbutylamine (33 mg, 0.22 mmol) dissolved in H_2O (5 mL) was added dropwise to the stirred hot solution and the mixture was allowed to cool down to room temperature. The clear colourless solution was kept in a plastic vial and after approximately 1 week colourless crystalline needles of **2** were isolated. The crystals were collected on a filter paper, washed with cold water and dried. Yield: 0.658 g (62 μmol, 36.7% based on W); characteristic IR bands: $\tilde{\nu} = 3315$ (m,br), 3049 (m), 1610 (w), 1471 (m), 1241 (w), 1051 (m), 1081 (vs), 985 (s), 951 (vs), 891 (vs), 785 cm^{-1} (s); elemental analysis calcd (%) for $C_{76}H_{238}N_{12}O_{170}W_{36}$: C 8.45, H 1.94, N 1.44, W 61.51; found: C 8.56, H 2.25, N 1.58, W 62.09.

Compound 3 ($(TEAH)_8Na_2\{(p(CH_2NH_3)_2C_6H_4))\subset[H_{12}W_{36}O_{120}]\}\cdot ca.17H_2O$): $Na_2WO_4\cdot 2H_2O$ (2.00 g, 6.06 mmol) and triethanolamine hydrochloride (2.5 g, 13.47 mmol) were dissolved in 50 mL H_2O and the pH was adjusted to 2.2 by using HCl (ca. 2 mL, 4 M). After heating the reaction mixture to 80 °C in a microwave, 14 mg (0.10 mmol) *p*XDA dissolved in H_2O (5 mL) was added dropwise to the stirred hot solution. The reaction mixture was allowed to cool to room temperature and the clear colourless solution was stored in a plastic vial. After 3–4 days, colourless crystalline needles of **3** were isolated. The crystals were collected on a filter paper and dried. Yield: 0.573 g (55 μmol, 32% based on W); characteristic IR bands: $\tilde{\nu} = 3450$ (m), 3150 (w), 1620 (w), 1474 (w), 1255 (w), 1201 (w), 1093 (s), 1065 (s), 1030 (s), 950 (vs), 898 (vs), 809 (s), 785 cm^{-1} (s); ^1H NMR (400 MHz, D_2O): $\delta = 7.61$ (brs, 4H), 4.20 (brs, 4H) 3.92 (m, 60H), 3.46 ppm (m, 60H); elemental analysis calcd (%) for $C_{56}H_{154}N_{10}Na_2O_{144}W_{36}$ (dried material): C 7.21, H 1.70, N 1.57, W 66.02, Na 0.25; found: C 6.76, H 1.56, N 1.41, W 66.63, Na 0.46.

Compound 4 ($(TEAH)_8Na_2\{(H_3N(C_6H_{12})NH_3)\subset[H_{12}W_{36}O_{120}]\}\cdot ca.17H_2O$): $Na_2WO_4\cdot 2H_2O$ (2.00 g, 6.06 mmol) and triethanolamine hydrochloride (2.5 g, 13.47 mmol) were dissolved in H_2O (50 mL). The solution pH was set to 2.2 by using HCl (ca. 2 mL, 4 M). After heating the reaction mixture to 80 °C in a microwave oven, 1,6-diaminohexane (23 mg, 0.20 mmol) dissolved in H_2O (5 mL) was added dropwise to the stirred hot solution and the mixture was allowed to cool down to room temperature. The clear colourless solution was kept in a plastic vial and after approximately 4 days colourless crystalline needles of **4** were isolated. The crystals were collected on a filter paper, washed with cold water and dried. Yield: 0.760 g (73 μmol, 43% based on W); characteristic IR bands: $\tilde{\nu} = 3438$ (m,br), 3065 (w), 1614 (w), 1448 (w), 1395 (w), 1320 (m), 1256 (m), 1205 (m), 1092 (m), 1066 (s), 985 (vs), 950 (vs), 890 (s), 781 cm^{-1} (s); ^1H NMR (400 MHz, D_2O): $\delta = 3.94$ (m, 60H), 3.48 (m, 60H) 3.10 (m, 2H), 1.81 (brs, 2H), 1.45 (brs, 2H); elemental analysis calcd (%) for $C_{54}H_{158}N_{10}O_{144}W_{36}$ (dried material): C 7.34, H 1.75, N 1.64, W 65.71, Na 0.23; found: C 6.53, H 1.61, N 1.41, W 66.76, Na 0.46.

Acknowledgement

This work was supported by the EPSRC and The University of Glasgow.

[1] D.-L. Long, E. M. Burkholder, L. Cronin, *Chem. Soc. Rev.* **2007**, *36*, 105; L. Cronin, High Nuclearity Polyoxometalate Clusters in Comprehensive Coordination Chemistry 2, 7th ed., **2004**, p. 1; M. T. Pope, A. Müller, *Angew. Chem.* **1991**, *103*, 56; *Angew. Chem. Int. Ed. Engl.* **1991**, *30*, 34; C. L. Hill, *Chem. Rev.* **1998**, *98*, 1.

[2] K. Wassermann, M. H. Dickman, M. T. Pope, *Angew. Chem.* **1997**, *109*, 1513; *Angew. Chem. Int. Ed. Engl.* **1997**, *36*, 1445; D.-L. Long, Y.-F. Song, E. F. Wilson, P. Kögerler, S.-X. Guo, A. M. Bond, J. S. J.

Hargreaves, L. Cronin, *Angew. Chem.* **2008**, *120*, 4456; *Angew. Chem. Int. Ed.* **2008**, *47*, 4384.
[3] L. Cronin, C. Beugholt, E. Krickemeyer, M. Schmidtmann, H. Bögge, P. Kögerler, T. K. K. Luong, A. Müller, *Angew. Chem.* **2002**, *114*, 2929; *Angew. Chem. Int. Ed.* **2002**, *41*, 2805.
[4] A. Müller, E. Beckmann, H. Bögge, M. Schmidtmann, A. Dress, *Angew. Chem.* **2002**, *114*, 1210; *Angew. Chem. Int. Ed.* **2002**, *41*, 1162.
[5] I. V. Kozhevnikov, *Chem. Rev.* **1998**, *98*, 171.
[6] J. T. Rhule, W. A. Neiwert, K. I. Hardcastle, B. T. Do, C. L. Hill, *J. Am. Chem. Soc.* **2001**, *123*, 12101.
[7] A. Müller, M. Luban, C. Schröder, R. Modler, P. Kögerler, M. Axenovich, J. Schnack, P. Canfield, S. Bud'ko, N. Harrison, *ChemPhysChem* **2001**, *2*, 517.
[8] A. Müller, P. Kögerler, A. W. M. Dress, *Coord. Chem. Rev.* **2001**, *222*, 193; L. Cronin, P. Kögerler, A. Müller, *J. Solid State Chem.* **2000**, *152*, 57.
[9] D. M. Way, A. M. Bond, A. G. Wedd, *Inorg. Chem.* **1997**, *36*, 2826; N. Fay, A. M. Bond, C. Baffert, J. F. Boas, J. R. Pilbrow, D.-L. Long, L. Cronin, *Inorg. Chem.* **2007**, *46*, 3502.
[10] P. J. S. Richardt, J. M. White, P. A. Tregloan, A. M. Bond, A. G. Wedd, *Can. J. Chem.* **2001**, *79*, 613; C. Streb, D.-L. Long, L. Cronin, *Chem. Commun.* **2007**, 471.
[11] H. D. Zeng, G. R. Newkome, C. L. Hill, *Angew. Chem.* **2000**, *112*, 1841; *Angew. Chem. Int. Ed. Engl.* **2000**, *39*, 1772.
[12] F. Ogliaro, S. P. de Visser, S. Cohen, P. K. Sharma, S. Shaik, *J. Am. Chem. Soc.* **2002**, *124*, 2806; Y.-F. Song, H. Abbas, C. Ritchie, N. McMillian, D.-L. Long, N. Gadegaard, L. Cronin, *J. Mater. Chem.* **2007**, *17*, 1903.
[13] D.-L. Long, H. Abbas, P. Kögerler, L. Cronin, *Angew. Chem.* **2005**, *117*, 3481; *Angew. Chem. Int. Ed.* **2005**, *44*, 3415; Y.-F. Song, N. McMillan, D.-L. Long, J. Thiel, Y. Ding, H. Chen, N. Gadegaard, L. Cronin, *Chem. Eur. J.* **2008**, *14*, 2349–2354; H. N. Miras, D.-L. Long, P. Kögerler, L. Cronin, *Dalton Trans.* **2008**, 214.
[14] K. F. Aguey-Zinsou, P. V. Bernhardt, U. Kappler, A. G. McEwan, *J. Am. Chem. Soc.* **2003**, *125*, 530.
[15] D. A. Judd, J. H. Nettles, N. Nevins, J. P. Snyder, D. C. Liotta, J. Tang, J. Ermolieff, R. F. Schinazi, C. L. Hill, *J. Am. Chem. Soc.* **2001**, *123*, 886.
[16] C. Streb, C. Ritchie, D.-L. Long, P. Kögerler, L. Cronin, *Angew. Chem.* **2007**, *119*, 7723; *Angew. Chem. Int. Ed. Engl.* **2007**, *46*, 7579; P. Kögerler, L. Cronin *Angew. Chem.* **2005**, *117, 866; Angew. Chem. Int. Ed.* **2005**, 44, 844; *Angew. Chem. Int. Ed.* **2005**, *44*, 844.
[17] D. Hagrman P. J. Hagrman J. Zubieta, *Angew. Chem.* **1999**, *111*, 3359; *Angew. Chem. Int. Ed.* **1999**, *38*, 3165; S. S. Kuduva N. Avarvari M. Fourmigue, *J. Chem. Soc. Dalton Trans.* **2002**, 3686.
[18] P. Mialane, A. Dolbecq, L. Lisnard, A. Mallard, J. Marrot and F. Secheresse, *Angew. Chem.* **2002**, *114*, 2504; *Angew. Chem. Int. Ed.* **2002**, *41*, 2398.
[19] T. Hori O. Tamada S. Himeno, *J. Chem. Soc. Dalton Trans.* **1989**, 1491; S. Juraja, T. Vu, P. J. S. Richardt, A. M. Bond, T. J. Cardwell, J. D. Cashion, G. D. Fallon, G. Lazarev, B. Moubaraki, K. S. Murray, A. G. Wedd, *Inorg. Chem.* **2002**, *41*, 1072.
[20] M. T. Pope in *Comprehensive Coordination Chemistry, Vol. 3* (Eds. G. Wilkinson, R. D. Gillard, J. A. McCleverty), Pergamon Press, **1987**.
[21] D.-L. Long, P. Kögerler, L. J. Farrugia, L. Cronin, *Angew. Chem.* **2003**, *115*, 4312; *Angew. Chem. Int. Ed.* **2003**, *42*, 4180; D.-L. Long, P. Kögerler, L. J. Farrugia, L. Cronin, *Dalton Trans.* **2005**, 1372.
[22] B. J. S. Johnson, R. C. Schroden, C. Zhu, A. Stein, *Inorg. Chem.* **2001**, *40*, 5972; M. Vasylyev, R. Popovitz-Biro, L. J. W. Shimon, R. Neumann, *J. Mol. Struct.* **2003**, *656*, 27.
[23] D.-L. Long, P. Kögerler, L. Cronin, *Angew. Chem.* **2004**, *116*, 1853; *Angew. Chem. Int. Ed.* **2004**, *43*, 1817; C. Fleming, D.-L. Long, N. McMillan, J. Johnson, N. Bovet, V. Dhanak, N. Gadegaard, P. Kögerler, L. Cronin, M. Kadodwala, *Nat. Nanotechnol.* **2008**, *3*, 229.
[24] D.-L. Long, D. Orr, G. Seeber, P. Kögerler, L. J. Farrugia, L. Cronin, *J. Cluster Sci.* **2003**, *14*, 313.
[25] H. Abbas, A. L. Pickering, D.-L. Long, P. Kögerler, L. Cronin, *Chem. Eur. J.* **2005**, *11*, 1071.
[26] H. Abbas, C. Streb, A. L. Pickering, A. R. Neil, D.-L. Long, L. Cronin, *Cryst. Growth Des.* **2008**, *8*, 635.
[27] J. J. Hastings, O. W. Howarth, *J. Chem. Soc. Dalton Trans.* **1992**, 209.
[28] S. Himeno, I. Kitazumi, *Inorg. Chim. Acta* **2003**, *355*, 81.
[29] D.-L. Long, H. Abbas, P. Kögerler, L. Cronin, *J. Am. Chem. Soc.* **2004**, *126*, 13880.
[30] D.-L. Long, O. Brücher, C. Streb, L. Cronin, *Dalton Trans.* **2006**, 2852.
[31] C. J. Pedersen, *J. Am. Chem. Soc.* **1967**, *89*, 7017.
[32] CCDC-691395 (**1**), 691396 (**2**), 691397 (**3**) and 691398 (**4**) contain the supplementary crystallographic data for this paper. These data can be obtained free of charge from The Cambridge Crystallographic Data Centre via www.ccdc.cam.ac.uk/data_request/cif.

Received: June 23, 2008
Published online: September 9, 2008

